Advances in Technology Innovation, vol. 9, no. 2, 2024, pp. 143-155

Influence of Surface Roughness on Durability of New-Old Concrete Interface

Nurdeen Mohamed Altwair*, Younis Omran Yacoub, Abdualhamid Mohamed Alsharif, Lamen Saleh Sryh

Department of Civil Engineering, El-Mergib University, Al-Khums, Libya

Received 01 April 2024; received in revised form 29 April 2024; accepted 30 April 2024

DOI: https://doi.org/10.46604/aiti.2024.13533

Abstract

The bond zone between old and new concrete is greatly affected by environmental factors. This study investigates the impact of surface roughness on durability using as-cast surface (CS), drilled holes surface (DS), and grooved surface (GS). After a 28-day water-curing, specimens undergo a 5% NaCl solution immersion for 30 and 60 days; exposure to temperatures of 200 ℃ and 500 ℃; and a water permeability test. Slant shear and splitting tensile tests assess durability. Results show that CS exhibits the greatest decrease in resistance to sodium chloride solution and temperature, while DS and GS show less pronounced effects. At 500 ℃, CS and DS specimens fail, whereas GS retains 50% and 75% of its shear and tensile strengths, respectively. GS has the lowest water permeability (7×10^{-11} m/s), followed by DS (1.2×10^{-10}) and CS (1.5×10^{-10}). Overall, surface roughness enhances durability and mitigates environmental effects.

Keywords: bonding strength, temperature, NaCl solution, permeability

1. Introduction

Repairing and strengthening structures often involves adding new concrete to an existing concrete substrate. Typically, before applying the concrete, the surface of the substrate is intentionally made rough. Numerous methods are evidenced to enhance surface roughness, with one of them being the mechanical approach. Tools like scarifiers, grinders, or shot blasting machines are frequently adopted to create a surface by removing the layer of the existing substrate and exposing the aggregate [1]. This rough texture promotes bonding between the old concrete, enabling mechanical methods to be highly effective in enhancing bonding.

The roughness of the existing substrate is particularly crucial in strengthening the bond between the new concrete [2]. A rough surface provides a contact area for the concrete to adhere to, resulting in improved bond strength. Additionally, it enables interlocking between both layers of concrete, further enhancing their bond strength. In other words, enhancing the roughness of the concrete substrate surface leads to improved interfacial bond strength, primarily attributed to increased interfacial shear friction and mechanical interlocking between the layers of concrete [3]. Previous research has examined techniques for creating surface roughness on concrete and improving bonding with newly applied concrete. The aforementioned methods were employed to roughen surfaces in real-world applications including utilizing a steel brush to prepare the surface, partially chipping the surface through holes, sandblasting the surface, and creating a textured surface [3-4].

The identification and characterization of bond qualities between old and new concrete have elicited considerable advances in structural engineering research in recent years. Nevertheless, the strength of the connection often serves as a critical area in repaired structures. Despite the progress herein, several ongoing concerns about the durability of bonding

* Corresponding author. E-mail address: nmaltwair@elmergib.edu.ly

English language proofreader: Chih-Wei Chang

systems emerge subsequently [4]. One particular concern is the insufficient understanding and investigation concerning bond deterioration in harsh environments [5]. Structural engineers delve into the durability of the bond zone between newly applied and existing concrete surfaces [6]. However, this zone is highly vulnerable to aggressive environmental conditions, especially after undergoing a rehabilitation period. The presence of chloride salts, acids, carbonation, significant variation in temperature and humidity, and the recurrence of freezing and thawing, can all contribute to the development of cracks that spread into undamaged regions [7], which ultimately compromises the overall durability of the concrete structure and may lead to structural failure.

Various environmental factors are evidenced, which can impact the durability of the bonding between existing and new concrete. Among these factors, elevated temperatures, chloride exposure, and water permeability are known to significantly affect the integrity of the interface [8]. The surface roughness of the old concrete substrate has been identified as an important parameter influencing the properties. The temperature resistance of the interface is a critical factor. The thermal stresses experienced by the interface between new and old concrete can induce detrimental effects, subsequently leading to cracking and, ultimately, failure [9-10].

Another significant concern regarding the new and old concrete interfaces is chloride resistance [11]. Coastal regions and construction sites that are exposed to deicing salts are more susceptible to the penetration of chloride. The penetration of chlorides into the concrete may exacerbate and expedite the corrosion of reinforcement, presenting a significant hazard to the structural durability of the whole system [7, 11]. Furthermore, the water permeability of the interface directly impacts the overall durability of the concrete structure [12]. The ingress of moisture through the interface can lead to various forms of damage, including freeze-thaw cycles and chemical degradation [13].

Previous studies have investigated the impact of various environmental factors on the bond strength between old concrete and repaired concrete. The studies conducted by Ding et al. [12] and Mallat and Alliche [14] expound on the importance of substrate roughness in enhancing the water impermeability and bond strength of concrete-based composites. While Ding et al. [12] observed marginally higher permeability coefficients in bonded self-healing concrete (SHC) with normal concrete (NC) compared to monotonic strain-hardening cementitious composite (SHCC), the overall improvement in splitting tensile strength indicated that the roughened surfaces and epoxy bonding effectively strengthened the interfacial bond between the two SHC and NC. Similarly, Tayeh et al. [2] explained the improved performance of ultra-high-performance concrete (UHPC)-NC composites, emphasizing mechanical interlock due to substrate roughening and the growth of hydration products as key factors contributing to the formation of a mechano-chemical bond. This bond, in turn, reduces the permeability of the composite to water, gas, and chloride ions.

On the other hand, Sabah et al. [15] conducted a retrospective study to investigate the composite action between UHPC and NC under fire exposure. The study employed various tests, including pull-off, flexure, splitting cylinder, and slant shear tests, to assess the bond strength between the two materials. The findings indicated an overall decrease in bond strength values across all test types. However, samples with roughened surfaces exhibited better performance and retained relatively higher strengths, particularly in tests involving tensile stresses.

In a more recent investigation by Gao et al. [10], the bond strength between Engineered cementitious composites (ECC) and high-strength (HS) overlays was studied under temperatures ranging up to 800 ℃. Interestingly, the researchers reported an anomalous result at 200 ℃, where an increase in bond strength was observed. Such phenomenon can be attributed to the availability of free water at the interface, which facilitates the hydration of unreacted cement grains. However, at temperatures beyond 600 ℃, the HS overlay experienced severe cracking, rendering it unendurable to any loads. In contrast, the ECC overlay still displayed small bond strength values, highlighting the remarkable ability of ECC to maintain its integral bond and cohesiveness with another concrete surface even after exposure to extremely high temperatures.

Regarding concrete bonding, significant progress has been achieved in understanding the quality of the bond between old and new concrete. Nonetheless, the paucity of comprehensive research on the durability of the bonding zone has not been resolved as yet. Existing studies have mainly focused on techniques to enhance the bonding, such as creating surface roughness, whereas scarce studies have addressed the influence of environmental factors on the bond. This research gap is particularly evident when considering the effects of temperature, direct exposure to chloride salt solutions, and water penetration on the contact area between the old and new concrete. These environmental factors can incur cracks and deterioration in the interface, compromising the overall durability of the repaired structure. To address this gap, further rigorous academic research is required to comprehensively understand the impact of these environmental conditions on the contact area and bond strength, especially in scenarios where the surface roughness of the old concrete changes, and the repaired concrete has normal compressive strength.

The primary objective of this study is to determine the optimal methods of surface roughness preparation, e.g., as-cast surface (CS), drilled holes surface (DS), and grooved surface (GS), that promote optimal bonding between existing and new concrete. Furthermore, the research aims to evaluate how this specific roughness influences permeability, ensures resistance against chloride salt attacks and enhances resistance against debonding when exposed to non-conventional temperature variations. To achieve these goals, the study will address the following tasks:

(1) Examine the effect of chloride salt solution and varying temperatures on the bond strength between existing and new concrete through slant shear and splitting tensile tests

(2) Assess the failure modes resulting from slant shear and splitting tensile tests when joint surfaces with different surface roughness between existing and new concrete are exposed to a sodium chloride salt solution and temperature

(3) Explore the influence of the concrete substrate surface with different surface roughness on reducing water penetration and improving the impermeability of the bond interface

2. Materials and Methods

Concrete was comprised of Portland cement, natural sand from the Zlitan region, and crushed gravel as coarse aggregate. The sand had a fineness modulus of 2.7, a specific gravity of 2.66, and a water absorption ratio of 0.85%. Crushed gravel was deployed as coarse aggregate with a maximum grain size of 19 mm, a density of 2.67 g/cm^3, and a water absorption of 2.8%. The process involved using ordinary tap water for curing and mixing fresh concrete, which exhibited qualities including freshness, potability, absence of color, taste, and biological materials. The composite specimens are composed of the concrete substrate and a newly designed concrete mixture intended to achieve normal-strength characteristics. Specifically, the NC was targeted to have a grade of 30 MPa. The specimens were prepared with a mix containing 396 kg/m^3 of cement, 185 kg/m^3 of water, 425 kg/m^3 of fine aggregate, and 1344 kg/m^3 of coarse aggregate.

This study focuses on preparing concrete surfaces before applying overlay concrete. The test specimens consist of two identical layers of concrete: the existing plain concrete substrate (old concrete) and the new concrete overlay. The plain concrete substrate specimens are placed within a lubricated mold and allowed to remain in their molds at room temperature for 24 hours. After a 24 hours period, the plain concrete substrate specimens are thoroughly cleaned and subjected to a 28-day curing process in a water curing tank. After 28 days of being cast and cured in water, the specimens were removed from the water tank for surface preparation. Three methods of preparing the concrete substrate surface were used: CS (without surface preparation), GS, and DS, as shown in Fig. 1. Before applying the new concrete overlay, the old concrete specimens were fully immersed in water for one day and subjected to a drying period of 25 minutes. Subsequently, the specimens were placed into their respective molds, and then the new concrete overlay was poured and allowed to cure at room temperature for 24 hours. After 24 hours, the specimens were removed from the molds and subjected to water curing for 28 days.

(a) As-cast surface (b) Drilled holes surface (c) Grooves

Fig. 1 Surface preparation

After curing for 28 days, the specimens were removed from the water curing tank immersed in NaCl solutions with mass concentrations of 5% for 30 and 60 days, and subjected to slant shear and splitting tensile tests. The slant shear specimens were designed with a prism shape measuring 15 cm × 15 cm × 30 cm (Fig. 2(a)). The specimens were tested under compression using the standard approach for assessing the compressive strength of cubes, as outlined in the ASTM C882 standard [16]. The splitting tensile test was based on the guidelines specified in BS EN 12390-6 [17]. As illustrated in Fig. 2(b), the specimens were modified from their original cylindrical shape to cubic specimens measuring 15 cm × 15 cm × 15 cm. In the particular experimental setup, using cubic specimens elicits the feasibility and efficiency to conduct a larger number of tests within the given time and resource constraints. Notably, both the cylinder-splitting test and the cube-splitting test yielded almost the same accuracy.

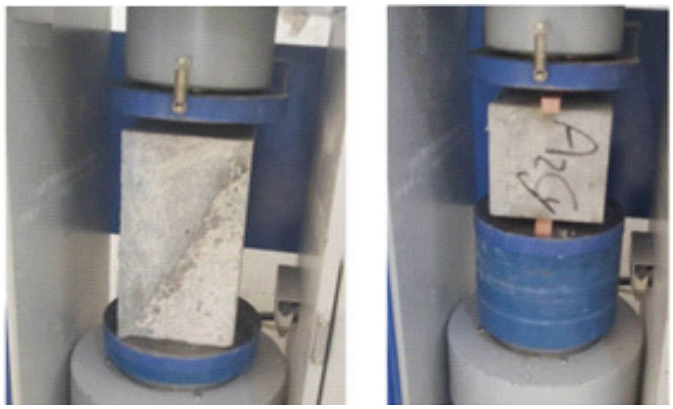

(a) Slant shear test (b) Splitting tensile test

Fig. 2 Test setup

An automatic electric furnace was used for the heating of specimens with a constant heating rate of about 15 ℃/min to reach the prescribed 200 ℃ and 500 ℃ temperature levels (Fig. 3). The temperature inside the furnace was maintained constant for three hours to achieve the thermal steady state condition after the target temperature was reached. After heating, the specimens were left at room temperature for one day before slant shear and splitting tensile tests.

Fig. 3 An automatic electric furnace contains specimens

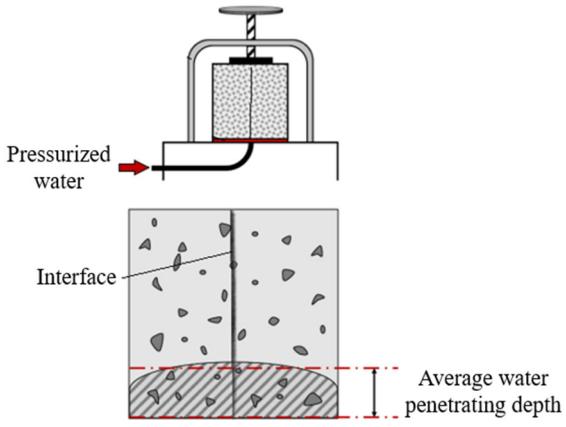

Fig. 4 Schematic view of permeability test

A water permeability test was conducted using cubic specimens with dimensions of 15 cm × 15 cm × 15cm, following BS EN 12390-8 [18]. The permeability testing procedure is schematically shown in Fig. 4. The test specimens were first placed inside the permeability cells, and then water was introduced on the lower face of the specimen. Meanwhile, a pressure head of 5.5 bars was applied in a direction parallel to the contact surface between the old and new concrete for 72 hours. Subsequently, the specimen was split in half perpendicular to the water pressure applied to the face. The maximum depth of penetration under the test area was recorded and measured to the nearest millimeter.

The coefficient of water permeability, k_w, was calculated using [19]:

$$k_w = \frac{d^2 v}{2ht} \tag{1}$$

where k_w is the coefficient of water permeability (in m/s); d is the depth of penetration of concrete in meters; h is the hydraulic head in meters; t is the time under pressure in seconds; and v is the porosity of concrete, which was determined following [2].

$$v = \frac{m}{Ad\rho} \tag{2}$$

where m is the gain in mass (in kg); A is the cross-sectional area of the specimen (in m^2); ρ is the density of water.

3. Results and Discussion

This section presents and discusses the results of the accelerated environmental exposure tests conducted. The analysis and discussion of the tests carried out in this part are organized as follows: Firstly, a comprehensive examination of the test results was performed, with a particular focus on the effect of subjecting the specimens to a sodium chloride solution. This part encompasses evaluations such as slant shear and splitting tensile tests. Subsequently, the analysis and discussion of the results obtained from exposing the samples to different temperatures are addressed using the same set of evaluations. Lastly, the analysis proceeds to discuss the results derived from the permeability test.

3.1. Effect of NaCl solution

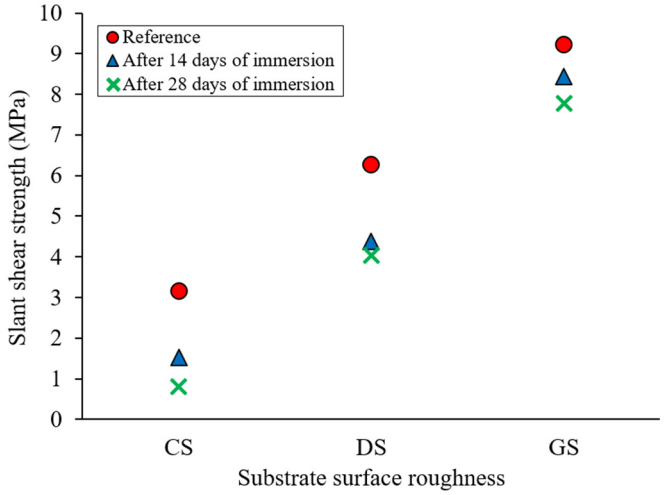

Fig. 5 The relationship between shear strength and surface roughness after 15 and 30 days of NaCl solution exposure

The slant shear test is a widely recognized method for measuring bond strength under combined compression and shear loads. Given its frequent deployment, moreover, it has been formally acknowledged by numerous international standards. Fig. 5 displays the experimental slant shear strength test results. It can be noted that the bond strength of specimens without a

roughening CS was found to decrease by 51% and 75% after 30 and 60 days when immersed in NaCl solution. Meanwhile, the DS specimens experienced a reduction of around 30% and 35% after 15 and 30 days, respectively. The GS specimens experienced a drop of around 8.6% and 15%.

The GS yielded a lower decrease in shear strength compared to other surface roughness methods. The GS exhibited an 81% and 90% increase in shear strength compared to the CS after 30 and 60 days of immersion in NaCl solution, respectively. The improvement also embodied a growth of around 49% to 48% compared to the DS at the corresponding ages. The ACI 546R-96 [20] specifies a minimum permissible slant bond strength ranging from 6.9 to 12 MPa. DS and GS indicated shear strengths within acceptable limits before being placed in NaCl solution. Furthermore, it was reported that the GS specimens, while being submerged in a NaCl solution for 60 days, exhibited shear strengths that fell within acceptable limits. These findings demonstrate that surfaces with varying types of roughness, such as DS and GS, significantly enhance the slant bond strength of the specimens in comparison to the control specimens.

The splitting tensile test is a method used to assess bond strength at composite interfaces and measure the indirect tensile strength of the composite interface. The splitting tensile test results are shown in Fig. 6 and are eminently consistent with those of the slant shear test. Furthermore, the results reflect that substrate surfaces significantly increased the indirect tensile capacity before submerging the specimens in NaCl solution. However, the DS and GS specimens demonstrated durability to the effects of the NaCl solution, particularly the grooved specimens, which provided the highest value of tensile strength after being submerged in a NaCl solution for 30 and 60 days. The groove method of surface preparation is the optimally efficient technique, as it yields the greatest capacity for indirect tensile strength compared to other methods. Quantitative bond quality can be classified into five categories based on bond strength as follows: excellent (> 2.1 MPa), very good (1.7-2.1), good (1.4-1.7), fair (0.7-1.4), and poor (0-0.7).

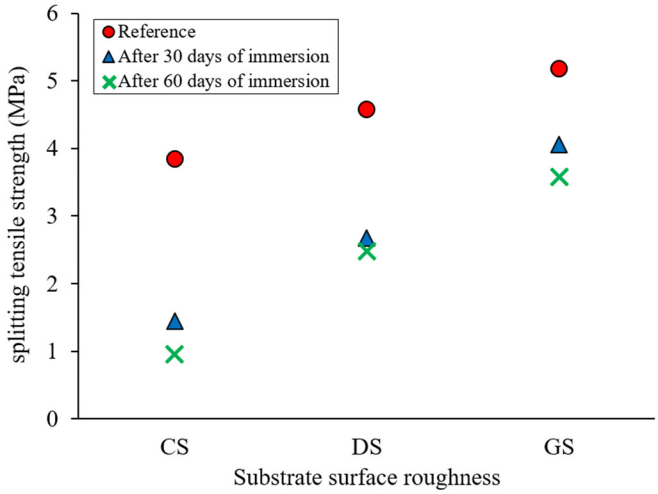

Fig. 6 The relationship between the splitting tensile strength and surface roughness after 15 and 30 days of NaCl solution exposure

Both DS and GS may be categorized as possessing exceptional bond strength since the bond strengths were more than 2.1 MPa. Furthermore, the findings concerning the impact of surface roughness were discovered to be highly consistent with those of Tayeh et al. [2], where the authors investigated various surface preparation methods for bonding ultra-high-performance fiber concrete to NC substrates to create repair composites. The researchers conducted a rapid chloride permeability test to evaluate the chloride resistance of the composites. Five different surface textures were employed for surface roughening, including no roughness, sandblasting, wire brushing, drilling holes, and creating grooves. The results highlight the significance of surface preparation in achieving a strong mechanical bond between the composites and the substrate. The composites that underwent surface treatment exhibited the highest mechanical bond strength, yielding an enhanced resistance against chloride penetration.

The application of sodium chloride to concrete induces a sequence of reactions and interactions. Given that sodium chloride would readily dissolve in water, the formation of sodium ions (Na^+) and chloride ions (Cl^-) can naturally react. Upon the dissociation of chloride ions from sodium ions, they gain mobility within the aqueous solution, enabling them to permeate the concrete matrix through capillary action and diffusion. They can migrate through voids, pores, and weak areas, such as the surface between old and new concrete. High concentrations of chloride ions can interfere with the hydration process of cement, disrupting the formation of the cementitious gel, and resulting in reduced strength and increased permeability [21].

Furthermore, grooves on the surface of old concrete (GS substrate) improve the bond strength with new concrete due to several factors. They provide interlocking mechanisms that enhance the mechanical connection between the layers, prevent slippage, increase the surface area available for bonding, facilitate chemical adhesion and mechanical interlocking, create a keying effect, distribute stresses between the old and new concrete, and help in load transfer by distributing stresses more uniformly [22]. The unique resistance of rough surfaces, especially those with GS, to the effects of NaCl solution, may be due to the presence of grooves creating a more complex and interlocking surface profile. This mechanical interlocking provides additional resistance against separation and increases the overall surface area available for bonding.

3.2. Effect of elevated temperature

The effect of temperature on the slant shear bond is shown in Fig. 7. The slant shear strength level was found to be susceptible to temperature changes. As shown in the figure, surface roughness is of evident importance in resisting the effects of temperature. By comparing the methods used in surface treatment, GS, yielded the highest slant shear strength, whether at a temperature of 200 ℃ or 500 ℃. The resistance of all the examined specimens to the effects of elevated temperature was observed at 200 ℃.

The CS and DS specimens, however, failed at 500 ℃, whereas the GS specimen remained resistant. Additionally, it is observed that the bonding strength of CS and DS decreased as the temperature increased due to the expansion emerging between the two layers of concrete and the development of thermal cracks on the composite surface, which also begot spelling at 500 ℃. The results of the slant shear strength of CS, DS, and GS were 0.87, 3.67, and 6.73 MPa at 200 ℃, respectively, while the slant shear strength of GS was 4.63 MPa at 500 ℃.

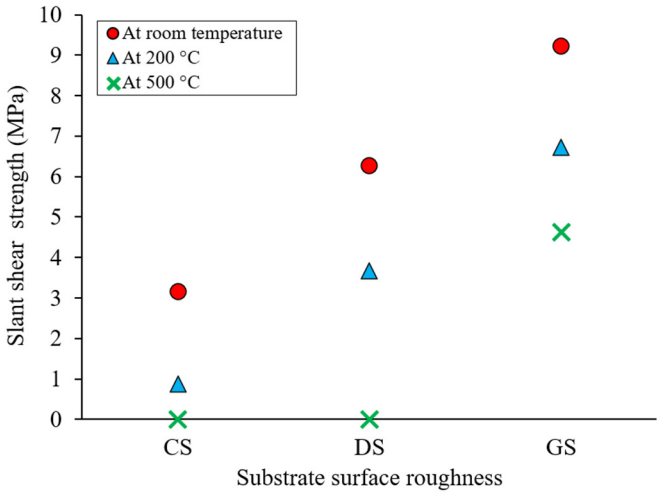

Fig. 7 The relationship between shear strength and surface roughness of specimens at 200 °C and 500 °C after 28 days of water curing

Failure patterns emerging during a slant shear strength test can be classified into four categories: pure interfacial failure (type A), concrete substrate cracking (type B), interfacial failure in conjunction with substrate fracture (type C), and substratum failure with a good interface (type D) [15]. Encapsulate from the slant shear test results of this study, at 200 ℃, all specimens with both CS and DS surface treatments were successfully categorized as failure mode type A, while the failure

mode in the GS, whether at 200 ℃ or 500 ℃, was type B (Fig. 8). Furthermore, despite being subjected to temperatures significantly exceeding the average room temperature, the GS specimens exhibited satisfactory strength, as specified in the ACI 546R-96 [20].

(a) CS exhibited type A (b) DS exhibited type A (c) GS exhibited type B

Fig. 8 Failure modes of specimens subjected to a slant shear test after exposure to temperature

Fig. 9 depicts the splitting tensile strength of specimens with varying roughness after exposure to temperatures of 200 and 500 ℃. The results of this test are consummately consistent with the scenarios concerning the slant shear test results. Observably, the percentage reduction in splitting tensile strength for CS, DS, and GS at 200 ℃ was 50%, 47%, and 14%, respectively.

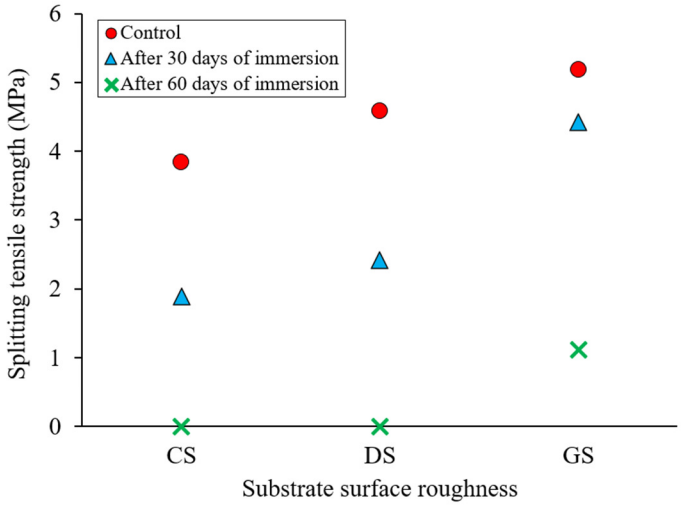

Fig. 9 The relationship between splitting tensile strength and surface roughness of specimens at 200 ℃ and 500 ℃ after 28 days of water curing

However, both CS and DS failed before the specified duration of the test when exposed to a temperature of 500 ℃, which is due to the development of thermal cracks on the composite surface and the decomposition of the concrete structure after exposure to high temperatures, physically and chemically, which begot spelling [15]. The splitting tensile strength of GS specimens experienced a decline of approximately 75%, which is deemed acceptable for withstanding the impact of such temperatures. The tensile bond strengths of specimens treated with GS at 500 ℃ ranged from 0.7 to 1.4 MPa (i.e., 1.12 MPa), indicating that the quality of bonding was satisfactory [2].

Indeed, the findings of this study correspond to the results reported by Behforouz et al. [23] in the related study. The study investigated the effects of fly ash content and surface preparation methods on the bond strength of repaired concrete subjected to high temperatures. To evaluate the effects, four surface preparation methods were employed: CS, wire brushed, grooved, and grooved-wire brushed. The findings revealed that surface preparation yielded the most significant influence on bond

strength, gradually improving the bond strength. In the case of overlay concretes without fly ash, the bond strength reached zero for the CS and wire-brushed surface preparation methods at temperatures of 400 ℃ and 600 ℃, respectively. Conversely, for the grooved and grooved-wire brushed methods, a 63% reduction was found in bond strength.

Based on Fig. 10, the failure mode of the studied specimens in the splitting tensile test is similar to the failure in the slant shear test. In other words, at 200 ◦C, the CS and DS specimens had interface fractures, and no damage was observed either from the substrate (old concrete) or the overlay concrete (new concrete). Total specimen failure occurred when the crack in the specimens subjected to tensile stresses emerged from the middle of the interface, propagated on both sides and reached the top and bottom of the specimens.

(a) CS exhibited type A (b) DS exhibited type A (c) GS exhibited type B

Fig. 10 Failure modes of specimens subjected to a splitting tensile test after exposure to temperature

Fig. 10(a) depicts the CS specimen subjected to the splitting tensile test. It can be observed that the concrete surface remained undamaged, and no additional damage was found on the surfaces (exhibiting type A failure). Fig. 10(b) illustrates DS specimens that underwent the splitting tensile test. During the test, a small portion of concrete was penetrated the cavities formed by the drilling process. The interface failure mode occurred between the surfaces, similar to CS specimens, which exhibited type A failure. Fig. 10(c) demonstrates the failure mode of the GS specimen under splitting tensile stress. The specimens had mixed-mode failure, which means minor substrate failure and interface failure occurred in specimens that exhibited type B failure.

Fig. 10(c) also reveals that the grooves provided significantly stronger bond strength compared to the substrate. It is palpable that the failure occurred partially within the substrate without complete separation or debonding between the substrate and the overlay concrete. The failure within the concrete substrate indicates robust bond proficiency, signifying that the strength of the interfacial bond is more significant than the strength of the concrete substrate. As stated by Hager [24], specimens exposed to a temperature of 500 ℃ consistently exhibit a gradual decrease in their bonding strength. This decrease is attributed to the rapid decline in the content of portlandite as it undergoes decomposition. Castellote et al. [25] further support this observation, reporting that the increase in CaO content in cement paste at 500 ℃ can be explained by the decomposition reaction of portlandite.

3.3. Water permeability evaluation

Fig. 11 depicts the water permeability of specimens with different surface treatments after 28 days of water curing. From this figure, it is evident that the surface roughness of the concrete substrate after treatment is the main factor affecting the permeability of the interface.

As presented in Fig. 11, it portrays that GS specimens exhibit a low value of water permeability, followed by DS specimens. It was found that the permeability coefficient was 1.5×10^{-10}, 1.2×10^{-10}, and 7×10^{-11} m/s for CS, DS, and GS, respectively. The percentage reduction in permeability coefficient values was approximately 20% for DS and 53% for GS compared to the permeability of CS. The grooved interface GS exhibits optimal impermeability due to its high interfacial

bonding strength, which effectively reduces water permeability. The GS specimens effectuate a high roughness of the interface, which can effectively improve the mechanical interlocking and chemical force of the interface [26]. However, the permeability coefficient values for GS specimens still fall within the range of water permeability coefficients typically observed in concrete with average quality (10^{-11} - 10^{-12} m/s) [27].

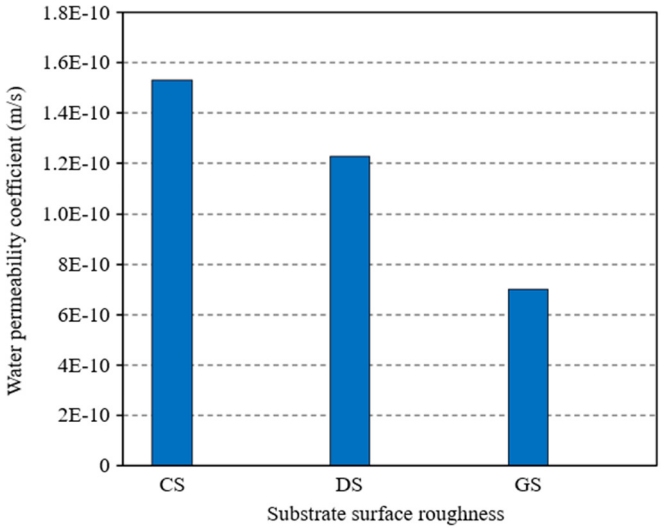

Fig. 11 Water permeability of specimens with varying roughness after 28 days of water curing

Fig. 12 demonstrates that the permeability of the bond interface between old and new concrete is influenced by the treatments applied to the interface. The black line in the figures represents the water penetration depth of the specimen's cross-section. When the interface is adequately treated and results in a well-bonded surface combination, the impermeability is significantly improved, effectively preventing water penetration.

Additionally, Fig. 12 illustrates that specimens with different roughness, particularly GS specimens, demonstrated resistance to water penetration in comparison to specimens without roughness. The depth of water penetration was lowest in GS specimens, then DS specimens, and finally CS specimens. As previously mentioned, the reason for the prevention of water penetration on rough surfaces, particularly in GS specimens, can be attributed to the presence of grooves that create a more intricate and interlocking surface profile. When water comes into contact with the bonding zone, the grooves enhance the mechanical interlocking between the layers. These grooves introduce irregularities that amplify frictional forces, producing more bonding strength. This mechanical interlocking significantly contributes to additional resistance against water penetration.

(a) As-cast surface (b) Drilled holes surface (c) Grooves

Fig. 12 Water penetration depth front marked after the test

Moreover, the grooves generate additional contact points and increase the surface area, facilitating a larger bonding interface. This increased surface area enhances bond strength and fortifies the resistance to water penetration [22]. This finding is in agreement with the explanation given by Ding et al. [12], who investigated the effects of interface treatment on the bonding surface permeabilities of SHCC and NC. Three surface treatments were used: no surface treatment, brushed interface,

and corrugated interface. The study found that the substrate material's influence on interface permeability depends on surface roughness. The bonding behavior between SHCC and NC is affected by factors such as existing concrete strength and surface roughness. The average permeability coefficient for the bonding surface treated by brushing was the lowest at 1.69×10^{-12} m/s, followed by the corrugated interface at 3.98×10^{-12} m/s. The bonding surface without treatment effectuated the highest average permeability coefficient at 7.81×10^{-12} m/s. These findings suggest that surface roughness is rather crucial in interfacial bonding strength and permeability.

4. Conclusions

Based on the results obtained from the conducted experiments, the following conclusions can be drawn:

(1) CS specimens exhibited a significant decrease in bond strength (51% and 75% after 30 and 60 days, respectively) when exposed to NaCl solution. DS showed better resistance, with a smaller reduction (30% and 35% after 15 and 30 days, respectively). GS showed the highest increase in shear strength (81% and 90% after 30 and 60 days, respectively), surpassing CS and DS. The splitting tensile test results supported these findings, with DS and GS significantly enhancing indirect tensile capacity. GS specimens displayed the highest tensile strength, indicating their durability against NaCl solution effects.

(2) At 200 °C, the slant shear strength results were 0.87 MPa for CS, 3.67 MPa for DS, and 6.73 MPa for GS. Splitting tensile strength reductions were 50% for CS, 47% for DS, and 14% for GS. CS and DS specimens displayed interface fractures, while GS specimens exhibited mixed-mode failure. At 500 °C, CS and DS specimens failed, while GS specimens showed a decline in bonding shear strength. GS specimens demonstrated a significant reduction in splitting tensile strength, indicating a robust interfacial bond within the concrete substrate.

(3) GS specimens demonstrated the lowest water permeability, with a coefficient of 7×10^{-11} m/s, followed by DS specimens with a coefficient of 1.2×10^{-10} m/s. CS specimens showed the highest permeability at 1.5×10^{-10} m/s. The permeability coefficient values for GS specimens fell within the typical range for average-quality concrete. Depth of water penetration results supported these findings.

The study focused on three surface preparation methods (CS, DS, and GS) to assess interfacial bond strength and durability. However, excluding environmental factors, such as carbonation and freeze-thaw cycles, limits further discussions. The evaluation was limited to specific exposure periods, hindering long-term insights. Field studies and techniques like SEM and XRD could enhance the investigation. The study did not consider the influence of concrete mix designs or properties. Future research should explore the impact of different compositions, including aggregates and admixtures, on interfacial zone performance.

Abbreviations and Symbols

CS	As-cast surface (without surface preparation)		HS	High-strength
DS	Drilled holes surface		Na^+	Sodium ions
GS	Grooved surface		Cl^-	Chloride ions
NaCl	Sodium chloride		SEM	Scanning electron microscopy
SHC	Self-healing concrete		XRD	X-ray diffraction
NC	Normal concrete		ASTM	American Society for Testing and Materials
SHCC	Strain-hardening cementitious composite		BSI	British Standards Institution
UHPC	Ultra-high-performance concrete		k_w	Coefficient of water permeability
ECC	Engineered cementitious composites		v	Porosity of concrete

Conflicts of Interest

The authors declare no conflict of interest.

References

[1] B. Zhang, J. Yu, W. Chen, H. Liu, H. Li, and H. Guo, "Experimental Study on Bond Performance of NC-UHPC Interfaces with Different Roughness and Substrate Strength," Materials, vol. 16, no. 7, article no. 2708, April 2023.

[2] B. A. Tayeh, B. H. Abu Bakar, M. A. Megat Johari, and Y. L. Voo, "Mechanical and Permeability Properties of the Interface between Normal Concrete Substrate and Ultra High Performance Fiber Concrete Overlay," Construction and Building Materials, vol. 36, pp. 538-548, November 2012.

[3] P. M. D. Santos and E. N. B. S. Júlio, "Factors Affecting Bond between New and Old Concrete," ACI Materials Journal, vol. 108, no. 4, pp. 449-456, July 2011.

[4] E. N. B. S. Júlio, F. A. B. Branco, and V. D. Silva, "Concrete-to-Concrete Bond Strength. Influence of the Roughness of the Substrate Surface," Construction and Building Materials, vol. 18, no. 9, pp. 675-681, November 2004.

[5] A. R. Sreadha, C. Pany, and M. V. Varkey, "A Review on Seismic Retrofit of Beam-Column Joints," International Journal for Modern Trends in Science and Technology, vol. 6, no. 9, pp. 80-93, September 2020.

[6] Y. Zhang, P. Zhu, Z. Liao, and L. Wang, "Interfacial Bond Properties between Normal Strength Concrete Substrate and Ultra-High Performance Concrete as a Repair Material," Construction and Building Materials, vol. 235, article no. 117431, February 2020.

[7] B. A. Tayeh, B. H. Abu Bakar, and M. A. Megat Johari, "Characterization of the Interfacial Bond between Old Concrete Substrate and Ultra High Performance Fiber Concrete Repair Composite," Materials and Structures, vol. 46, no. 5, pp. 743-753, May 2013.

[8] D. Daneshvar, A. Behnood, and A. Robisson, "Interfacial Bond in Concrete-to-Concrete Composites: A Review," Construction and Building Materials, vol. 359, article no. 129195, December 2022.

[9] D. Daneshvar, K. Deix, and A. Robisson, "Effect of Casting and Curing Temperature on the Interfacial Bond Strength of Epoxy Bonded Concretes," Construction and Building Materials, vol. 307, article no. 124328, November 2021.

[10] S. Gao, X. Zhao, J. Qiao, Y. Guo, and G. Hu, "Study on the Bonding Properties of Engineered Cementitious Composites (ECC) and Existing Concrete Exposed to High Temperature," Construction and Building Materials, vol. 196, pp. 330-344, January 2019.

[11] Q. Chen, R. Ma, H. Li, Z. Jiang, H. Zhu, and Z. Yan, "Effect of Chloride Attack on the Bonded Concrete System Repaired by UHPC," Construction and Building Materials, vol. 272, article no. 121971, February 2021.

[12] Z. Ding, J. Wen, X. Li, and X. Yang, "Permeability of the Bonding Interface between Strain-Hardening Cementitious Composite and Normal Concrete," AIP Advances, vol. 9, no. 5, article no. 055107, May 2019.

[13] Y. Zhao, S. Lian, J. Bi, C. Wang, and K. Zheng, "Study on Freezing-Thawing Damage Mechanism and Evolution Model of Concrete," Theoretical and Applied Fracture Mechanics, vol. 121, article no. 103439, October 2022.

[14] A. Mallat and A. Alliche, "Mechanical Investigation of Two Fiber-Reinforced Repair Mortars and the Repaired System," Construction and Building Materials, vol. 25, no. 4, pp. 1587-1595, April 2011.

[15] S. H. Abo Sabah, N. L. Zainal, N. Muhamad Bunnori, M. A. Megat Johari, and M. H. Hassan, "Interfacial Behavior between Normal Substrate and Green Ultra-High-Performance Fiber-Reinforced Concrete under Elevated Temperatures," Structural Concrete, vol. 20, no. 6, pp. 1896-1908, December 2019.

[16] Standard Test Method for Bond Strength of Epoxy-Resin Systems Used with Concrete by Slant Shear, ASTM C882, 1999.

[17] Testing Hardened Concrete - Part 6: Tensile Splitting Strength of Test Specimens, BS EN 12390-6, 2009.

[18] Testing Hardened Concrete - Part 8: Depth of Penetration of Water Under Pressure, BS EN 12390-8, 2009.

[19] S. I. Ahmad, M. S. Rahman, and M. S. Alam, "Water Permeability Properties of Concrete Made from Recycled Brick Concrete as Coarse Aggregate," IOP Conference Series: Materials Science and Engineering, vol. 809, article no. 012015, 2020.

[20] Concrete Repair Guide, ACI 546R-96, 1996.

[21] J. Liu, K. Tang, D. Pan, Z. Lei, W. Wang, and F. Xing, "Surface Chloride Concentration of Concrete under Shallow Immersion Conditions," Materials, vol. 7, no. 9, pp. 6620-6631, September 2014.

[22] I. De La Varga, J. F. Muñoz, D. P. Bentz, R. P. Spragg, P. E. Stutzman, and B. A. Graybeal, "Grout-Concrete Interface Bond Performance: Effect of Interface Moisture on the Tensile Bond Strength and Grout Microstructure," Construction and Building Materials, vol. 170, pp. 747-756, May 2018.

[23] B. Behforouz, D. Tavakoli, M. Gharghani, and A. Ashour, "Bond Strength of the Interface between Concrete Substrate and Overlay Concrete Containing Fly Ash Exposed to High Temperature," Structures, vol. 49, pp. 183-197, March 2023.

[24] I. Hager, "Behaviour of Cement Concrete at High Temperature," Bulletin of the Polish Academy of Sciences Technical Sciences, vol. 61, no. 1, pp. 145-154, 2013.

[25] M. Castellote, C. Alonso, C. Andrade, X. Turrillas, and J. Campo, "Composition and Microstructural Changes of Cement Pastes upon Heating, as Studied by Neutron Diffraction," Cement and Concrete Research, vol. 34, no. 9, pp. 1633-1644, September 2004.

[26] J. Fan, L. Wu, and B. Zhang, "Influence of Old Concrete Age, Interface Roughness and Freeze-Thawing Attack on New-to-Old Concrete Structure," Materials, vol. 14, no. 5, article no. 1057, March 2021.

[27] F. Rendell, R. Jauberthie, and M. Grantham, Deteriorated Concrete: Inspection and Physicochemical Analysis, London: Thomas Telford, 2002.